



Cite this: *Chem. Sci.*, 2022, **13**, 2202

Received 15th November 2021  
Accepted 23rd December 2021

DOI: 10.1039/d1sc06315d  
[rsc.li/chemical-science](http://rsc.li/chemical-science)

## 1. Introduction

Cellular redox homeostasis, which refers to the dynamic balance between intracellular oxidizing species and reducing

<sup>a</sup>Department of Medical Ultrasound, Shanghai Tenth People's Hospital, Tongji University, Tongji University Cancer Center, Tongji University School of Medicine, Shanghai, P. R. China

<sup>b</sup>Department of Materials Science and State Key Laboratory of Molecular Engineering of Polymers, Fudan University, Shanghai, P. R. China. E-mail: [lvguanglei@fudan.edu.cn](mailto:lvguanglei@fudan.edu.cn); [wbbu@fudan.edu.cn](mailto:wbbu@fudan.edu.cn)

<sup>c</sup>Key Laboratory of Molecular Target and Clinical Pharmacology & the State Key Laboratory of Respiratory Disease, School of Pharmaceutical Sciences & the Fifth Affiliated Hospital, Guangzhou Medical University Guangzhou, P. R. China

† These authors contributed equally to this work.



*Yelin Wu received his PhD degree from East China Normal University. He is now a professor at Tongji University Cancer Center, Shanghai Tenth People's Hospital. His research interests focus on the design and application of nanomaterials for cancer and wound healing.*

species, plays an important role in maintaining normal physiological processes such as cell growth, metabolism, differentiation, aging and apoptosis.<sup>1</sup> Oxidizing species are a class of chemical substances that tend to obtain electrons from reducing agents in redox reactions, including reactive oxygen species (ROS),<sup>2</sup> reactive nitrogen species (RNS),<sup>3</sup> and so on. A moderate concentration of intercellular oxidizing species such as ROS is required for various biological processes including cell signaling, biosynthetic processes, and host defense.<sup>4</sup> However, excessive amounts of ROS can cause oxidative damage to lipids, proteins, and DNA, which leads to oxidative stress.<sup>5</sup> Under this persistent intrinsic oxidative stress, reducing species, a class of oxidizing species-scavenging substances, are activated to protect cells from ROS-induced oxidative damage.



*Yanli Li received her PhD degree in 2021 from the East China Normal University (ECNU), under the supervision of Prof. Wenbo Bu. She is now an associate professor at Guangzhou Medical University. Her research interests focus on the design and synthesis of multifunctional nanomaterials for biomedical applications.*



Therefore, it is crucial to keep cellular redox homeostasis for normal cell survival and growth.

Compared with normal cells, numerous types of cancer cells tend to elevate levels of oxidizing species owing to the genetic instability, increased chronic inflammation, and aberrant metabolism.<sup>6</sup> Oxidizing species in turn induce gene mutation and inflammation, leading to the generation of more oxidizing species.<sup>7</sup> This cycle ultimately results in persistent oxidative stress. Cancer cells that survive oxidative stress mobilize a set of adaptive mechanisms through enhancing antioxidant capacity.<sup>8,9</sup> This adaptive system contributes to malignant transformation, metastasis, and resistance of tumor cells to ROS-mediated tumor therapies such as part of chemotherapeutic drugs, radiotherapy (RT), photodynamic therapy (PDT), and chemodynamic therapy (CDT).<sup>4,10-12</sup> Therefore, it is crucial to disrupt tumor redox homeostasis to make tumor cells sensitive to current tumor treatment modalities.

The redox dyshomeostasis (RDH) strategy for tumor therapy is first proposed by our group, aiming to make tumor cells more sensitive to different tumor therapy patterns<sup>13</sup> through disrupting the cellular redox homeostasis using nanomaterials (Fig. 1). Unlike traditional chemotherapeutic drugs, nanomaterials have their special characteristics such as passive targeting, drug delivery, and tendency of losing or gaining electrons. Therefore, based on these characteristics, nanomaterials could be designed to modulate the redox homeostasis of tumor cells by delivering and reacting with oxidizing or reducing species, under endogenous stimuli such as low pH and hypoxia, or external stimuli such as light and ultrasound.<sup>14</sup> Here, this review summarizes the most recent progress of the nanomaterial-based RDH strategy for novel and efficient tumor therapies, mainly including the following regulations to realize RDH: (1) regulation of oxidizing species; (2) regulation of reducing species, and (3) regulation of both oxidizing species and reducing species.

## 2. Regulation of oxidizing species to realize RDH

Oxidizing species mainly include ROS and RNS. ROS are oxygen-containing molecules with higher chemical reactivity including superoxide anions ( $O_2^{\cdot-}$ ), hydrogen peroxide ( $H_2O_2$ ), and

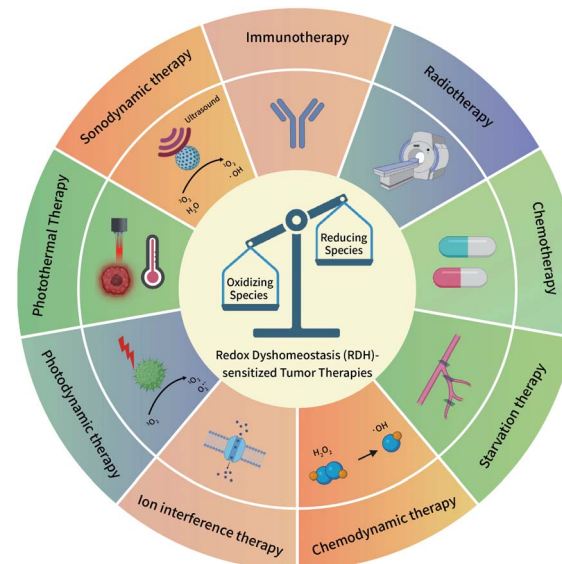


Fig. 1 A schematic overview of the redox dyshomeostasis (RDH) strategy for tumor therapy.

hydroxyl radicals ( $\cdot OH$ ). RNS are nitrogen-containing oxidants, mainly including nitric oxide (NO) and peroxynitrite ( $ONOO^{\cdot-}$ ). Among these oxidizing species,  $H_2O_2$  is a significantly stable and diffusible form of ROS.<sup>9</sup> Furthermore, as an intermediate product of mammalian oxygen metabolism,  $H_2O_2$  is easily transformed into various active species in cells.<sup>6</sup> Therefore,  $H_2O_2$  is one of the most important oxidizing species, which is capable of being regulated to disrupt redox homeostasis. In the past few years, a series of nanomaterials have been constructed to increase  $H_2O_2$  production, realizing the RDH strategy to enhance the sensitivity of tumor therapy. On the basis of working principles, increasing the  $H_2O_2$  level can be realized through two distinctive strategies: (1) biosynthesis approaches; (2) chemical approaches.

### 2.1 Increasing the $H_2O_2$ level in tumor cells *via* biosynthesis approaches

$H_2O_2$  can be generated in tumor cells through biosynthesis approaches.<sup>4,6</sup> For example, electron leakage from the



Guanglei Lv received his PhD degree from Fudan University under the supervision of Prof. Tao Yi. Then, he worked as a lecturer at Zhejiang Normal University until 2020. He is now working as a postdoctoral researcher in the group of Prof. Wenbo Bu at Fudan University. His current research interests focus on the design and synthesis of organic/inorganic materials and their bio-applications.



Wenbo Bu received his PhD degree from Nanjing University of Technology. He is a full professor at Fudan University and an adjunct professor at Chinese Academy of Sciences (SICCAS). His current research interests include the design and synthesis of multifunctional nanomaterials for cancer imaging and therapeutic applications.



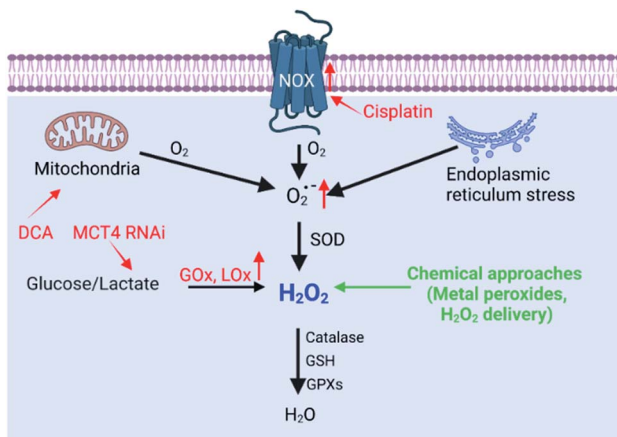


Fig. 2 Biosynthesis and strategies of increasing  $\text{H}_2\text{O}_2$  via biosynthesis approaches and chemical approaches (red font represents biosynthesis approaches and green font represents chemical approaches).

mitochondrial respiratory chain or endoplasmic reticulum (ER) stress can promote  $\text{H}_2\text{O}_2$  production. In addition, the production of  $\text{H}_2\text{O}_2$  is controlled by a series of biosynthesis-related enzymes, such as NADPH oxidase (NOX), glucose oxidase (GOx) and lactate oxidase (LOx) (Fig. 2). Therefore, enzymes, the function of mitochondria and ER, and the substrate ( $\text{O}_2$  and  $\text{O}_2^{\cdot-}$ ) have been regulated using a wide range of nanomaterials

to increase the  $\text{H}_2\text{O}_2$  level, realizing RDH to enhance the sensitivity of tumor therapy.  $\text{H}_2\text{O}_2$  production is driven by both enzyme-dependent and -independent strategies.

**2.1.1 Enzyme-dependent strategies.** NOX, the main  $\text{H}_2\text{O}_2$ -generating enzymes in eukaryotic cells, are closely associated with redox homeostasis.<sup>15</sup> It has been reported that cisplatin induces the production of ROS via NADPH oxidase activation in human prostate cancer cells.<sup>16</sup> Jun Lin *et al.* constructed self-sacrificing iron-oxide nanoparticles with cisplatin(IV) drug FePt-NP2. As shown in Fig. 3A, once the nanoparticles entered the cells, cisplatin was released to activate NOX, which catalyzed the formation of superoxide and  $\text{H}_2\text{O}_2$  from  $\text{O}_2$ . The accumulation of  $\text{H}_2\text{O}_2$  disrupted redox homeostasis, leading to RDH in tumor cells. The RDH enhanced  $\text{Fe}^{2+}/\text{Fe}^{3+}$ -induced Fenton reaction resulted in tumor cell death.<sup>17</sup> GOx and LOx are the main producers of  $\text{H}_2\text{O}_2$  in prokaryotic cells. Among them, GOx can catalyze glucose to generate glucose acid and  $\text{H}_2\text{O}_2$ , and LOx can catalyze lactic acid to produce  $\text{H}_2\text{O}_2$ . Therefore, GOx and LOx are promising enzymes to increase the  $\text{H}_2\text{O}_2$  level, achieving RDH. Jianlin Shi *et al.* loaded GOx and ultra-small  $\text{Fe}_3\text{O}_4$  into macroporous silica nanoparticles (MSN) to prepare a biodegradable and sequentially functioning nanocatalyst GOx- $\text{Fe}_3\text{O}_4$ @DMSN. GOx catalyzed glucose into abundant  $\text{H}_2\text{O}_2$ , resulting in RDH in tumors, which promoted  $\text{Fe}_3\text{O}_4$  NP-induced Fenton-like reactions.<sup>18</sup> Similarly, Changfeng Wu constructed a nanoparticle platform by covalent conjugation of GOx to small

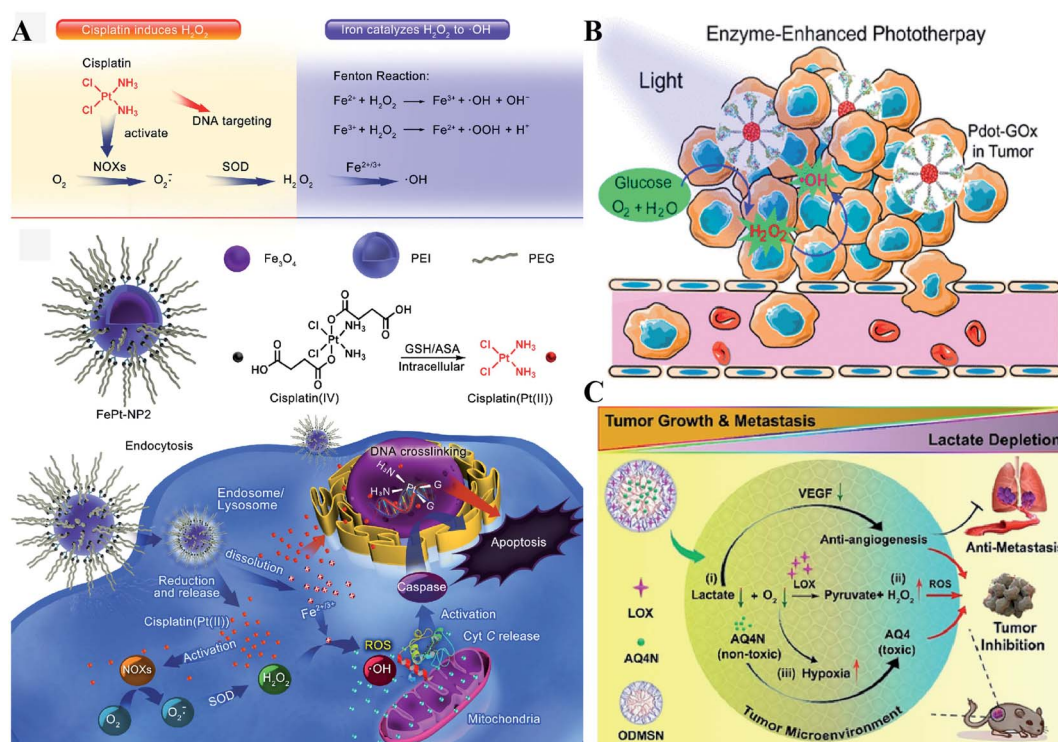


Fig. 3 Schematic illustrations of enzyme-dependent strategies to realize RDH. (A) Cisplatin from FePt-NP2 activated NOX to produce  $\text{H}_2\text{O}_2$  and then induced RDH, which sensitized  $\text{Fe}^{2+}/\text{Fe}^{3+}$ -induced cell death. Adapted from ref. 17 with permission. Copyright 2017 American Chemical Society. (B) GOx from Pdot-GOx catalyzed glucose oxidation to generate  $\text{H}_2\text{O}_2$  realizing RDH which enhanced phototherapy. Adapted from ref. 19 with permission. Copyright 2017 American Chemical Society. (C) LOx from ODMSN catalyzed lactate depletion and  $\text{H}_2\text{O}_2$  production. The latter induced RDH promoting AQN4-induced chemotherapy. Adapted from ref. 20 with permission. Copyright 2020 Wiley-VCH.



polymer dots. This nanosystem could be persistently immobilized into a tumor and catalyze glucose oxidation to generate  $H_2O_2$ , leading to RDH, which was beneficial for phototherapy (Fig. 3B).<sup>19</sup> Therefore, these examples indicate that RDH in tumor cells enhances the sensitivity of 'OH induced by the Fenton reaction or phototherapy. Besides GOx, Lox-catalyzed generation of  $H_2O_2$  has been used to disrupt redox homeostasis. Chengzhong Yu *et al.* reported a nanoplatform, where Lox and a chemotherapy drug AQ4N were loaded into open-work@dendritic mesoporous silica nanoparticles.<sup>20</sup> Lox catalyzed lactate depletion and  $H_2O_2$  production. The former downregulated VEGF expression and inhibited angiogenesis, while the latter induced RDH promoting AQN4-induced chemotherapy (Fig. 3C).

**2.1.2 Enzyme-independent strategies.** Besides enzyme-regulated  $H_2O_2$  production, the biosynthesis of  $H_2O_2$  can be regulated by the increase of substrates and enhanced metabolic processes.  $O_2$  and  $O_2^{.-}$  are the indispensable substrates for  $H_2O_2$  biosynthesis.  $O_2^{.-}$  can be produced by photosensitizers upon light excitation.<sup>21</sup> Xiaojun Peng *et al.* developed a near-

infrared light-triggered molecular superoxide radical generator (ENBS-B).<sup>22</sup> ENBS-B can produce a considerable amount of  $O_2^{.-}$ , which can be transformed to  $H_2O_2$  by SOD-mediated reactions. The increased  $H_2O_2$  induced RDH, promoting Fenton reaction and Haber-Weiss reaction-induced cancer cell apoptosis (Fig. 4A). Similarly, Haifeng Dong *et al.* synthesized metal-organic framework (MOF) nanosheets (DBBC-UiO), which were composed of 5,15-di(*p*-benzoato)bacteriochlorin ( $H_2DBBC$ ) as blocks and heavy  $Hf_6(\mu_3-O)_4(\mu_3-OH)_4$  clusters as centers.<sup>23</sup> This system could produce considerable  $O_2^{.-}$  under a hypoxic environment with 750 nm irradiation. The produced  $O_2^{.-}$  could not only kill tumor cells but transform to  $H_2O_2$  via SOD-mediated reactions. The robust  $H_2O_2$  induced the imbalance of redox homeostasis to realize RDH, which ultimately improved the PDT efficacy.

Altering lactic acid and energy metabolism can also trigger the production of  $H_2O_2$ .<sup>24</sup> The high rate of glycolysis in the tumor is associated with the excessive generation of lactic acid, which leads to the upregulation of MCT4,<sup>25</sup> an efflux of lactate/ $H^+$  for maintaining a stable intracellular pH and acidic tumor microenvironment. It has been reported that MCT4 silencing could block the intracellular lactate efflux, resulting in more  $H_2O_2$  production. Jinjun Shi *et al.* developed a unique amorphous iron oxide (AIO) MCT4 RNAi NP platform. Silencing of MCT4 induced the accumulation of  $H_2O_2$ , leading to RDH, which exacerbated the Fenton-like reaction for tumor treatment (Fig. 4B).<sup>26</sup> In addition, Xinghai Ning *et al.* used dichloroacetic acid (DCA) to increase mitochondrial aerobic oxidation for the production of  $H_2O_2$ .<sup>27</sup> They constructed a liposomal formulation MD@Lip containing DCA and MOF- $Fe^{2+}$ . DCA promoted the production of  $H_2O_2$  leading to RDH, which sensitized the MOF- $Fe^{2+}$ -associated antitumor strategy.

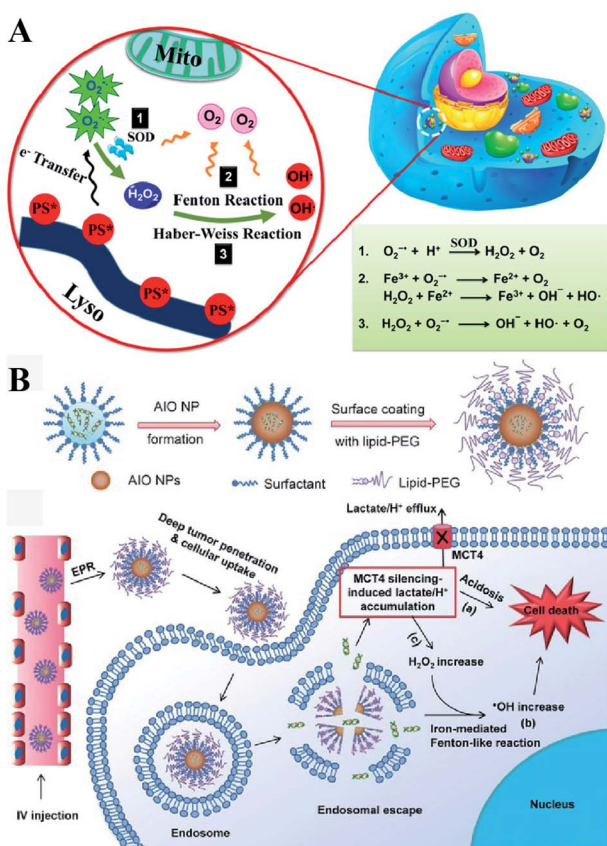


Fig. 4 Schematic illustrations of enzyme-independent strategies to induce RDH. (A) Near-infrared light triggered ENBS-B to produce a considerable amount of  $O_2^{.-}$  which is transformed to  $H_2O_2$  leading to RDH, promoting Fenton reaction and Haber-Weiss reaction-induced cell apoptosis. Adapted from ref. 22 with permission. Copyright 2018 American Chemical Society. (B) Silencing of MCT4 induced the accumulation of  $H_2O_2$ , which realized RDH, exacerbating Fenton-like reaction-mediated tumor treatment. Adapted from ref. 26 with permission. Copyright 2018 Wiley-VCH.

## 2.2 Increasing the $H_2O_2$ level in tumor cells *via* chemical approaches

Besides regulation of  $H_2O_2$  production *via* biosynthesis strategies, the most straightforward way to generate  $H_2O_2$  in tumor cells is to directly deliver or produce  $H_2O_2$  at tumor sites *via* chemical approaches. Compared with biosynthesis, chemical approaches can rapidly increase the  $H_2O_2$  content in a short time, leading to RDH. By ingeniously designing functional nanomaterials,  $H_2O_2$  can be produced in two ways: (1) direct delivery and (2) chemical reactions.

**2.2.1 Increasing the  $H_2O_2$  level in tumor cells by direct delivery.** Directly delivering  $H_2O_2$  into tumor cells is the most straightforward way to increase the  $H_2O_2$  content, resulting in RDH. Chen-Sheng Yeh *et al.* encapsulated  $H_2O_2$  into the  $Fe_3O_4$ -PLGA polymersome.<sup>28</sup> On exposure to ultrasound, the polymersome can be easily disrupted to release  $H_2O_2$ , causing RDH, which enhanced the  $Fe_3O_4$ -induced Fenton reaction (Fig. 5A). Similarly, in order to supply enough oxygen for enhanced radioimmunotherapy of cancer, Zhuang Liu *et al.* separately loaded  $H_2O_2$  and catalase (CAT) into stealthy liposomes.<sup>29</sup> The CAT@liposome was preinjected into tumor sites followed by  $H_2O_2$ @liposome injection. Therefore, the sustainably released  $H_2O_2$  of  $H_2O_2$ @liposome could be decomposed by the catalase



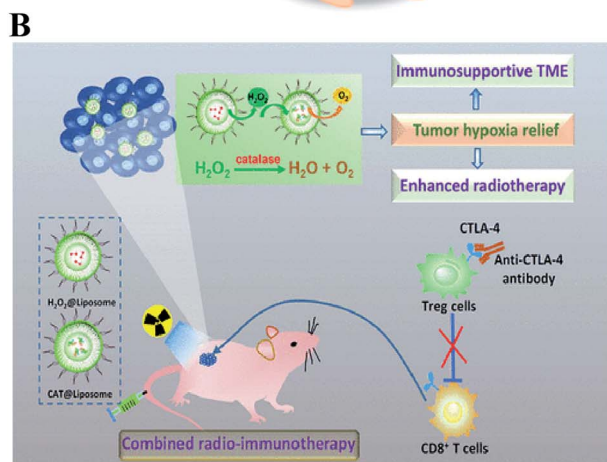
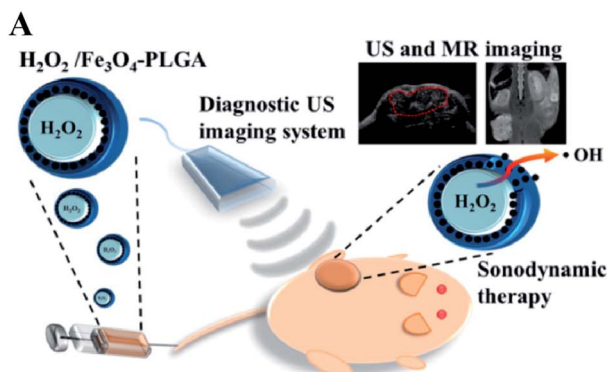


Fig. 5 Schematic illustrations of increasing the  $\text{H}_2\text{O}_2$  level in tumor cells by direct delivery. (A)  $\text{H}_2\text{O}_2/\text{Fe}_3\text{O}_4$ -PLGA polymersome-induced RDH. On exposure to ultrasound, the polymersome can be easily disrupted to release  $\text{H}_2\text{O}_2$ , causing RDH which enhanced the  $\text{Fe}_3\text{O}_4$ -induced Fenton reaction. Adapted from ref. 28 with permission. Copyright 2016 American Chemical Society. (B)  $\text{H}_2\text{O}_2$ @liposome and CAT@liposome-induced RDH. The sustainably released  $\text{H}_2\text{O}_2$  of  $\text{H}_2\text{O}_2$ @liposome could be decomposed by catalase from CAT@liposome, resulting in a long-lasting oxygen release and RDH, which enhanced the radiotherapy and immunotherapy. Adapted from ref. 28 with permission. Copyright 2018 American Chemical Society.

from CAT@liposome, resulting in a long-lasting oxygen release and RDH, which further enhanced the therapeutic effects of radiotherapy and CTLA4 (cytotoxic T lymphocyte-associated antigen 4) antibody-mediated immunotherapy (Fig. 5B).

**2.2.2 Increasing the  $\text{H}_2\text{O}_2$  level in tumor cells by chemical reactions.** Direct delivery of  $\text{H}_2\text{O}_2$  into tumor sites may have some disadvantages such as poor stability and uncontrollable action. Undoubtedly, producing  $\text{H}_2\text{O}_2$  *in situ* is a promising alternative. Metal peroxides are typically composed of metal ions and peroxy groups, which can react with  $\text{H}_2\text{O}$  to produce  $\text{H}_2\text{O}_2$  under acid conditions.<sup>30</sup> Therefore, metal peroxides are capable of specifically responding to the acidic tumor microenvironment to produce a large number of  $\text{H}_2\text{O}_2$  in tumor sites, which could disrupt the redox homeostasis of tumors and ultimately enhance the sensitivity of tumor cells to other treatments. For example, our group constructed a biodegradable nanoprodrug of transferrin-modified  $\text{MgO}_2$  nanosheets. In response to the acidic and low catalase activity of the tumor

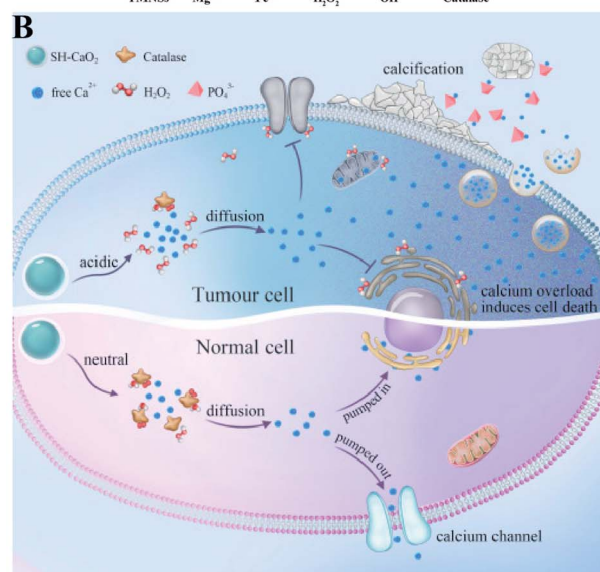
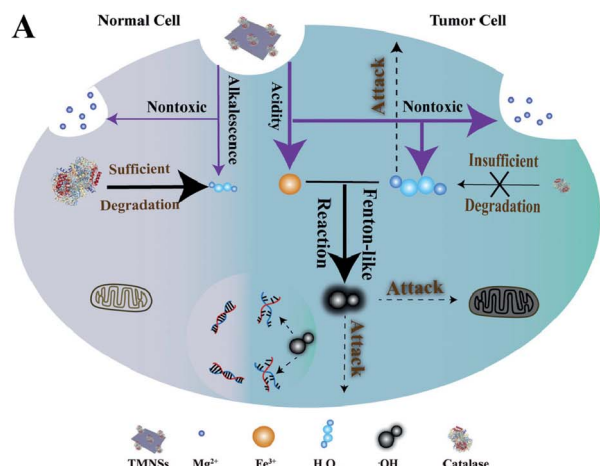


Fig. 6 Schematic illustrations of increasing the  $\text{H}_2\text{O}_2$  level by chemical reactions. (A)  $\text{MgO}_2$ -induced RDH.  $\text{MgO}_2$  nanosheets produced abundant  $\text{H}_2\text{O}_2$  to disrupt redox homeostasis enhancing transferrin-mediated CDT. Adapted from ref. 31 with permission. Copyright 2019 Wiley-VCH. (B)  $\text{SH-CaO}_2$ -induced RDH.  $\text{SH-CaO}_2$  produced abundant  $\text{H}_2\text{O}_2$  to disrupt redox homeostasis enhancing  $\text{Ca}^{2+}$ -mediated ion interference therapy (IIT). Adapted from ref. 33 with permission. Copyright 2019 Elsevier.

microenvironment,  $\text{MgO}_2$  produced abundant  $\text{H}_2\text{O}_2$  to disrupt redox homeostasis, ultimately enhancing transferrin-mediated CDT (Fig. 6A).<sup>31</sup> Similarly, Xiaoyuan Chen *et al.* reported a method of fabricating copper peroxide nanodots (CP).<sup>32</sup> The CP nanodots decomposed under the acidic environment of endo/lysosomes, allowing the simultaneous release of Fenton catalytic  $\text{Cu}^{2+}$  and  $\text{H}_2\text{O}_2$ . The increase of  $\text{H}_2\text{O}_2$  induced RDH, sensitizing  $\text{Cu}^{2+}$ -induced CDT. Altering the metal ion content balance could induce a series of intracellular responses, even cell death. This approach has been used to treat tumors and was defined as ion interference therapy (IIT).<sup>33</sup> For example, calcium ion ( $\text{Ca}^{2+}$ ) accumulation is a cause of damage or cell death in various cell types. With this in mind, we constructed pH-sensitive sodium-hyaluronate-modified calcium peroxide



nanoparticles (SH-CaO<sub>2</sub> NPs) to produce abnormal H<sub>2</sub>O<sub>2</sub> accumulation and calcium overload.<sup>33</sup> The increased level of H<sub>2</sub>O<sub>2</sub> disturbed cellular redox homeostasis and enhanced calcium overload-induced cell death (Fig. 6B). Taken together, these strategies combined RDH with CDT and IIT, opening a new door for further material design and corresponding tumor treatment.

### 2.3 Increasing other oxidizing species to realize RDH

Besides ROS, RNS including NO and ONOO<sup>−</sup> are another important oxidizing species. A few studies have been designed to produce RNS modulating the redox homeostasis of tumor cells. For example, our group constructed an intelligent X-ray-controlled NO-releasing upconversion nano-theranostic system PEG-USMSx-SNO. The increase of NO could induce RDH consequently sensitizing radiotherapy (Fig. 7A).<sup>34</sup> In order to achieve a better antitumor effect and inhibit tumor metastasis, Jun Lin *et al.* fabricated a multifunctional nano-vaccine based on L-arginine (LA)-loaded black mesoporous titania (BMT). By using ultrasound, BMT and LA were triggered to produce NO which not only induced RDH but also induced cell apoptosis through DNA double-strand breaks. All of these eventually enhanced PD-L1 antibody-mediated immunotherapy, further inhibiting metastatic tumors (Fig. 7B).<sup>35</sup>

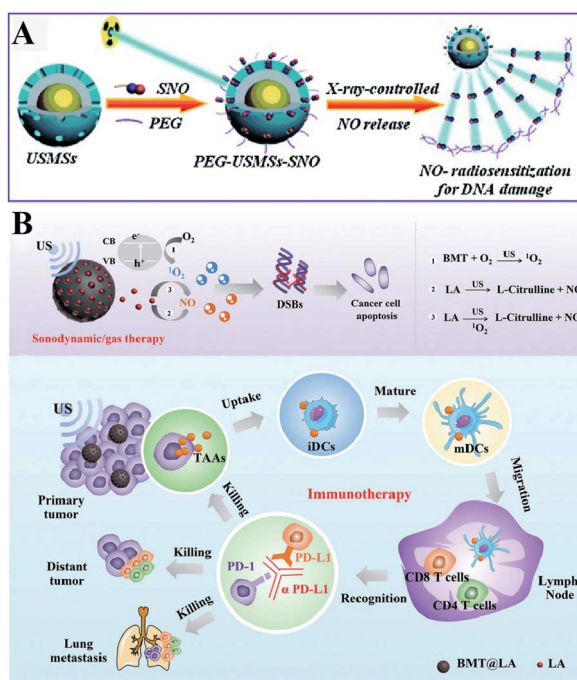


Fig. 7 Schematic illustrations of NO-induced RDH. (A) X-ray-controlled NO release induced RDH, sensitizing X-ray-mediated radiotherapy. Adapted from ref. 34 with permission. Copyright 2015 Wiley-VCH. (B) BMT and LA were triggered by ultrasound to produce NO, which induces RDH, sensitizing PD-L1 antibody-mediated immunotherapy. Adapted from ref. 35 with permission. Copyright 2021 Wiley-VCH.

## 3. Regulation of reducing species to realize RDH

To protect tumor cells from damage by oxidative stress, the powerful antioxidant defense system of cells maintains the balance of intracellular redox by producing reducing species.<sup>36</sup> Reducing species, as another part of redox homeostasis, essentially transfer electrons to oxidizing species, which would decrease the sensitivity of tumor cells to ROS-mediated tumor therapy. Therefore, inhibiting the production of reducing species could effectively break the redox balance and also promote the efficacy of tumors.<sup>37–41</sup> It is well established that glutathione (GSH) is the primary reducing species for intracellular ROS scavenging, and its presence significantly reduces intracellular ROS levels and weakens the effect of tumor therapy. Therefore, GSH is one of the most important reducing species capable of being regulated to disrupt redox homeostasis. Thus, how to reduce GSH to break the redox homeostasis of tumor cells is one of the cutting-edge research directions of the RDH strategy. In the past few years, numerous nanomaterials have been constructed to decrease GSH production,<sup>42,43</sup> adopting the RDH strategy to enhance the sensitivity of tumor therapy. Based on working principles, inhibition of GSH can be divided into two distinctive strategies: (1) suppressing GSH biosynthesis; (2) chemical approaches (Fig. 8).

### 3.1 Decreasing the GSH level of tumor cells to realize RDH via suppressing GSH biosynthesis

The biosynthesis of GSH consists of the production of GSH and the recycling of GSH. The process of GSH production includes the formation of  $\gamma$ -glutamylcysteine from glutamate and

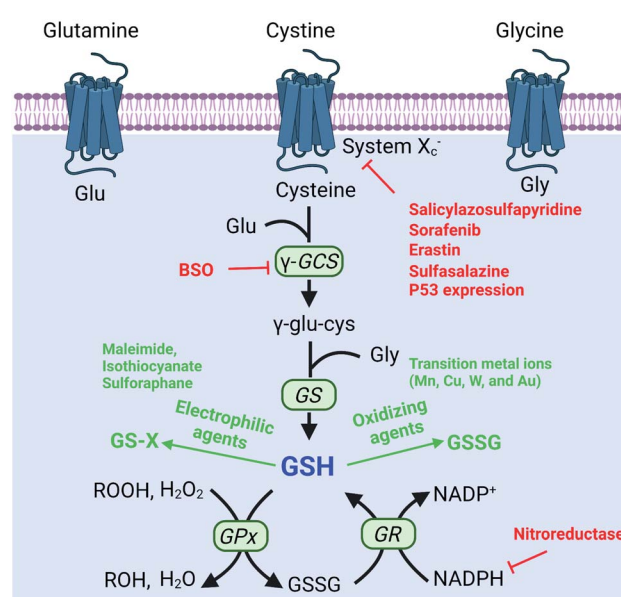


Fig. 8 Biosynthesis pathways of GSH and strategies of decreasing the GSH level via biosynthesis approaches and chemical approaches (red font represents biosynthesis approaches and green font represents chemical approaches).



cysteine, and the formation of GSH from  $\gamma$ -glutamylcysteine and glycine.<sup>44</sup> In this system, cysteine is an indispensable precursor for GSH.  $\gamma$ -glutamine cysteine synthase ( $\gamma$ -GCS) and GSH synthetase (GS) are two rate-limiting enzymes for the biosynthesis of GSH. After GSH production, GSH acts as an antioxidant to reduce hydrogen peroxide and lipid peroxide through GSH peroxidase (GPx)-catalyzed reactions. In this process, GSH is oxidized to oxidized-glutathione (GSSG). In turn, GSSG is reduced back to GSH by GSSG reductase (GR) at the expense of NADPH, thereby forming a redox cycle. Therefore, the biosynthesis level of GSH is dependent on synthesis-related enzymes ( $\gamma$ -GCS or GS), substances (cysteine, glutamate and glycine) and the recycling level (NADPH) (Fig. 8). Thus, with this knowledge, we conclude that nanomaterials have the potential to suppress GSH biosynthesis. The suppression of GSH is also driven by enzyme-dependent and -independent strategies.

**3.1.1 Enzyme-dependent strategies.**  $\gamma$ -GCS and GS are two important enzymes for the biosynthesis of GSH. However, compared with the overexpression of GS, the overexpression of  $\gamma$ -GCS could elevate higher levels of GSH. Therefore,  $\gamma$ -GCS is used as a more popular target for the regulation of GSH synthesis.<sup>45,46</sup> The  $\gamma$ -GCS inhibitor L-buthionine-(S,R)-sulfoximine (BSO) is the most widely used chemical compound for the inhibition of GSH biosynthesis.<sup>47</sup> Xiaolin Wang *et al.* developed

near-infrared photothermal liposomal nano-antagonists (PLANS) containing a photosensitizer indocyanine (ICG) and BSO. BSO inhibited GSH synthesis to disrupt redox homeostasis, amplifying ICG-mediated cancer PDT.<sup>48</sup> Similarly, Kun Zhang *et al.* constructed a tumor metabolism-engineered composite nanoplateform  $\text{Nb}_2\text{C}/\text{TiO}_2/\text{BSO-PVP}$ .  $\text{Nb}_2\text{C}$  was used to load  $\text{TiO}_2$  sonosensitizers and BSO. The loaded BSO can block GSH synthesis to break redox homeostasis, which can maximally increase SDT (Fig. 9A).<sup>49</sup>

**3.1.2 Enzyme-independent strategies.** In addition to enzyme-dependent strategies, the biosynthesis of GSH can be regulated by substrate availability and GSH recycling. Cysteine is the indispensable substrate for GSH biosynthesis.<sup>50–52</sup> However, cysteine is unstable in the cytosol of cells and easily oxidized to cystine. Therefore, uptake of stable cystine that is reduced to cysteine in cell cytosol is another rate-limiting step in GSH biosynthesis. Several transporters, such as cystine/glutamate transporter System  $\text{X}_\text{C}^-$  (SLC7A11 and SLC3A2), *P*-glycoprotein (*P*-gp, ABCB1), and breast cancer resistance protein (BCRP, ABCG2),<sup>14</sup> have been confirmed to be involved in the control of cysteine concentration. Among them, System  $\text{X}_\text{C}^-$  and its inhibitors (salicylazosulfapyridine,<sup>53</sup> sorafenib,<sup>54</sup> erastin,<sup>55</sup> and sulfasalazine<sup>56</sup>) have been broadly used to inhibit GSH biosynthesis. Ruijie Chen *et al.* reported a nanocomposite to inhibit the GSH synthesis, where  $\text{ZnO}$  nanoparticles (NPs) were used as a carrier, loaded with salicylazosulfapyridine (SASP) and stabilized with DSPE-PEG to form ultra-small NPs (SASP/ $\text{ZnO}$  NPs).<sup>53</sup> SASP was used to inhibit the transport function of SLC7A11, resulting in the decrease of cysteine for GSH synthesis. As a consequence, treatment of tumor cells with SASP/ $\text{ZnO}$  NPs resulted in a disruption of redox balance in tumor cells, enhancing  $\text{ZnO}$ -induced cell death (Fig. 9B). Similarly, sorafenib (SFB) could block the System  $\text{X}_\text{C}^-$  transport system to inhibit the biosynthesis of GSH.<sup>57,58</sup> With this in mind, Fanzhu Li *et al.* constructed targeted SFB loaded manganese-doped silica nanoparticles (FaPEG-MnMSN@SFB), which were capable of destroying the intracellular redox homeostasis by the consumption of GSH and the inhibition of GSH synthesis.<sup>54</sup> This strategy ultimately enhanced ROS-dependent ferroptosis. Apart from the  $\text{X}_\text{C}^-$  inhibitor, endogenous protein expression can also regulate SLC7A11 expression. It has been reported that the famous tumor suppressor gene P53 can inhibit cystine uptake by repressing the expression of SLC7A11.<sup>59</sup> Xianzheng Zhang *et al.* used a metal-organic network (MON) to encapsulate P53 plasmid (MON-P53). Once MON-P53 was internalized by cancer cells, the expression of P53 can inhibit the expression of SLC7A11 and then decrease the transport of cysteine for GSH synthesis. The decrease of GSH promoted RDH in tumor cells, increasing the sensitivity of cells to ferroptosis-mediated cell death.<sup>60</sup>

In the process of GSH recycling, GSSG can be in turn reduced back to GSH under the catalysis of NADPH and the GSH reductase (GR), which forms a redox cycle. Therefore, decreasing the level of NADPH may inhibit GSH production by breaking the redox cycle.<sup>43</sup> Yanjun Zhao *et al.* constructed a polymer containing hydrophilic poly(ethylene glycol) (PEG) that was linked by azobenzene with a nitroimidazole-

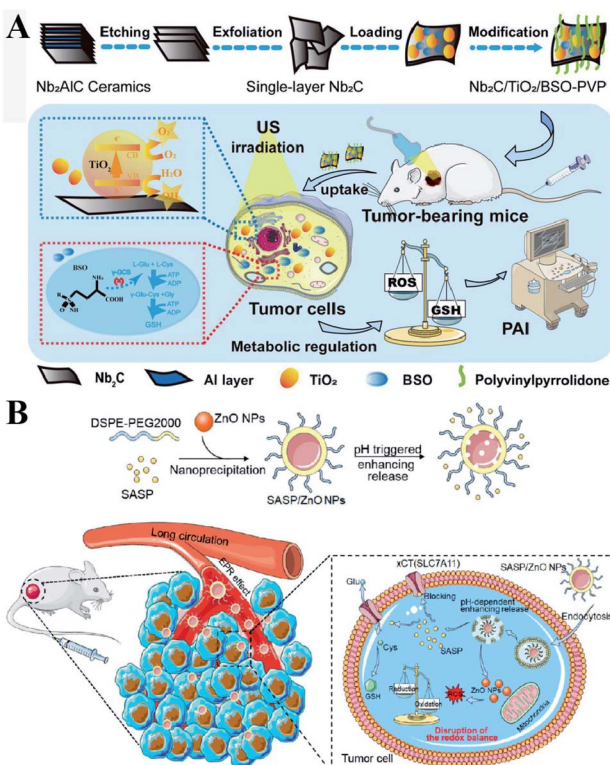


Fig. 9 (A) Schematic illustrations of the synthesis process and function of the Nb<sub>2</sub>C/TiO<sub>2</sub>/BSO-PVP. Adapted from ref. 49 with permission. Copyright 2020 Wiley-VCH. (B) Design and application of SASP/ZnO NPs for cancer therapy. Adapted from ref. 53 with permission. Copyright 2019 American Chemical Society.



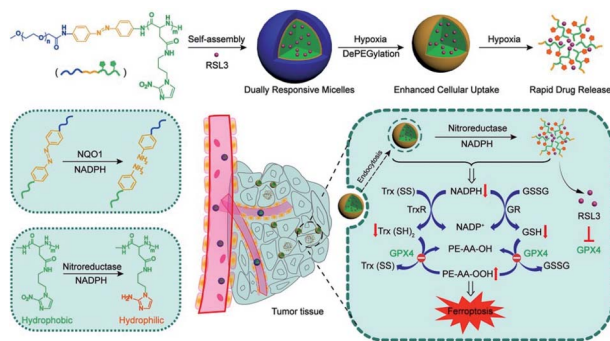


Fig. 10 Schematic illustrations of NADPH inhibition-mediated RDH. NADPH depletion diminished intracellular glutathione and thioredoxin, which destroyed tumor redox homeostasis enhancing the sensitivity of RSL3-induced ferroptosis. Reprinted from ref. 61 with permission. Copyright 2020 American Chemical Society.

conjugated polypeptide.<sup>61</sup> The nitroimidazole moiety was reduced by the overexpressed nitroreductase with reduced NADPH as the cofactor, resulting in transient depletion of NADPH. The lack of NADP impaired both the glutathione and thioredoxin redox cycle, leading to diminished intracellular glutathione and thioredoxin. As a result, tumor redox homeostasis was destroyed, which enhanced the sensitivity of RSL3-induced ferroptosis (Fig. 10). This RDH strategy *via* blocking

NADPH to decrease GSH is still less studied. Besides azobenzene, etomoxir, a carnitine palmitoyltransferase 1 inhibitor, can also decrease NADPH levels, thereby reducing the GSH content by inhibiting fatty acid oxidation.<sup>62</sup> Etomoxir has not been used for the construction of nanomaterials for RDH.

### 3.2 Decreasing the GSH level of tumor cells to realize RDH *via* chemical approaches

Decreasing GSH *via* biosynthesis approaches is an effective and specific strategy, but the underlying biological mechanisms and possible side effects require further study. Using chemical approaches to deplete GSH involves introducing some substances that can react with GSH. Compared with the suppression of GSH biosynthesis, chemical approaches are a more straightforward way. However, the function is temporary and short-lived, as tumor cells may increase the GSH level through alternative pathways. Currently, chemical approaches can be divided into two categories: (1) consumption of GSH by oxidizing agents, and (2) consumption of GSH by electrophiles.

**3.2.1 Consumption of GSH by oxidizing agents.** Converting GSH to GSSG using oxidizing agents is a rapid method to consume GSH. Oxidizing agents include transition metal (Mn, Cu, W, Mo, and Au) ions. Numerous research groups made extensive effort in this area. Weihong Tan *et al.* reported a smart chlorine 6 (Ce6)–manganese dioxide (MnO<sub>2</sub>) nano drug delivery

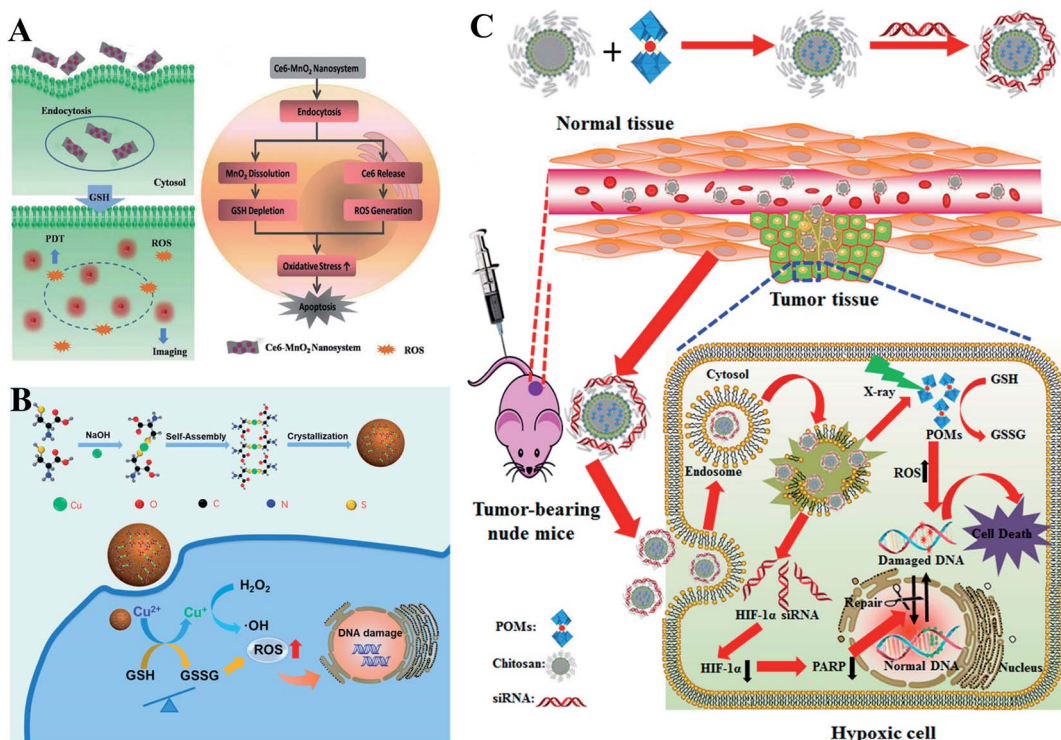


Fig. 11 Schematic illustrations of GSH depletion by oxidizing agents. (A) MnO<sub>2</sub> of the Ce6–MnO<sub>2</sub> nanosystem consumed GSH to induce RDH, thereby sensitizing photosensitizer Ce6-induced PDT effects. Adapted from ref. 63 with permission. Copyright 2016 Wiley–VCH. (B) Schematic illustrations of Cu-induced GSH depletion. Cu<sup>2+</sup> in Cu-Cys NPs consumed GSH to induce RDH and simultaneously generate Cu<sup>+</sup>. This RDH state of the cells was more sensitive to the cytotoxicity of Cu<sup>+</sup>-mediated CDT. Adapted from ref. 71 with permission. Copyright 2019 American Chemical Society. (C) W<sup>6+</sup> of GdW10@CS triggered GSH oxidation leading to RDH, thereby facilitating the efficiency of radiotherapy. Adapted from ref. 72 with permission. Copyright 2017 American Chemical Society.



system.<sup>63</sup>  $\text{MnO}_2$  consumed GSH to induce RDH, thereby sensitizing photosensitizer Ce6-induced PDT effects (Fig. 11A).  $\text{Mn}^{2+}$  could not only consume GSH but also display Fenton-like properties.<sup>64–66</sup> Based on this, Xiaoyuan Chen *et al.* constructed  $\text{MnO}_2$ -based mesoporous silica nanoparticles (MS@ $\text{MnO}_2$  NP).<sup>67</sup> Once taken up by cancer cells, the  $\text{MnO}_2$  shell was used to oxidize GSH to accumulate  $\text{H}_2\text{O}_2$ , which led to RDH, ultimately enhancing  $\text{Mn}^{2+}$ -mediated CDT. Compared with Mn ions,  $\text{Cu}^+$  displays higher efficacy of CDT.<sup>68–70</sup> Our group developed self-assembled copper-amino acid mercaptide nanoparticles (Cu-Cys NPs).<sup>71</sup>  $\text{Cu}^{2+}$  in Cu-Cys NPs was first reduced by local GSH to generate  $\text{Cu}^+$  and simultaneously realize GSH depletion, leading to RDH. Subsequently, this state of the cells was more sensitive to the cytotoxicity of  $\text{Cu}^+$ -catalyzed toxic  $\cdot\text{OH}$  (CDT). These cascade reactions can perfectly achieve “two birds with one stone” in cancer treatment (Fig. 11B). In addition, Yuliang Zhao *et al.* found that oxidative W(vi) also had the capacity to react with intracellular GSH in cancer cells.<sup>72</sup> They developed Gd-containing polyoxometalate-conjugated chitosan ( $\text{GdW}_{10}@\text{CS}$  nanosphere) as a radiosensitization system. The  $\text{GdW}_{10}@\text{CS}$  nanospheres were able to promote the depletion of intracellular GSH by synergy  $\text{W}^{6+}$ -triggered GSH oxidation. As a result, the as-synthesized  $\text{GdW}_{10}@\text{CS}$  nanospheres disrupted the redox homeostasis of tumor cells, thereby facilitating the efficiency of radiotherapy (Fig. 11C). To achieve more specific radiotherapy, they further explored bismuth heteropolytungstate ( $\text{BiP}_5\text{W}_{30}$ ) nanoclusters as radiosensitizers.<sup>73</sup> In this system,  $\text{BiP}_5\text{W}_{30}$  had the capability of depleting GSH *via* redox reaction owing to its unique electron structure and multi-electron properties. GSH consumption induced RDH, sensitizing high-Z elements like Bi and W-enhanced radiotherapy. In recent years, it has been widely reported that gold (Au) as a radiosensitizer can exhaust GSH by the formation of an Au-S bond, showing great promise in preclinical studies.<sup>74</sup> Wu *et al.* prepared histidine-capped gold nanoclusters (Au NCs@His) for GSH depletion and RDH, thereby sensitizing Au-mediated cancer radiotherapy.<sup>75</sup>

**3.2.2 Consumption of GSH by electrophiles.** Besides the use of oxidizing agents to deplete GSH, many electrophilic reagents that can directly react with thiol groups are also used to consume GSH, leading to the RDH of tumors. Compared with oxidizing agents, electrophilic reagents may non-selectively react with nucleophiles, leading to undesirable toxic effects. Therefore, moderately active electrophilic such as maleimide, isothiocyanate and sulforaphane were used to consume GSH. For example, Minjie Sun *et al.* developed maleimide liposome (ML) adjuvants to deplete GSH for augmenting the photothermal immunotherapy of breast cancer.<sup>76</sup> The maleimide group of ML can irreversibly react with thiols of GSH by Michael addition. The depletion of GSH caused RDH, enhancing photothermal immunotherapy of breast cancer through promoting immunogenic cell death (ICD) and dendritic cell maturation (Fig. 12). In addition, Xiangliang Yang *et al.* employed a natural compound,  $\beta$ -phenylethyl isothiocyanate (PEITC), found in cruciferous vegetables, to deplete intracellular GSH through the formation of the conjugate of PEITC with GSH.<sup>77</sup> They combined ICG-loaded hydroxyethylstarch-oleic acid conjugate

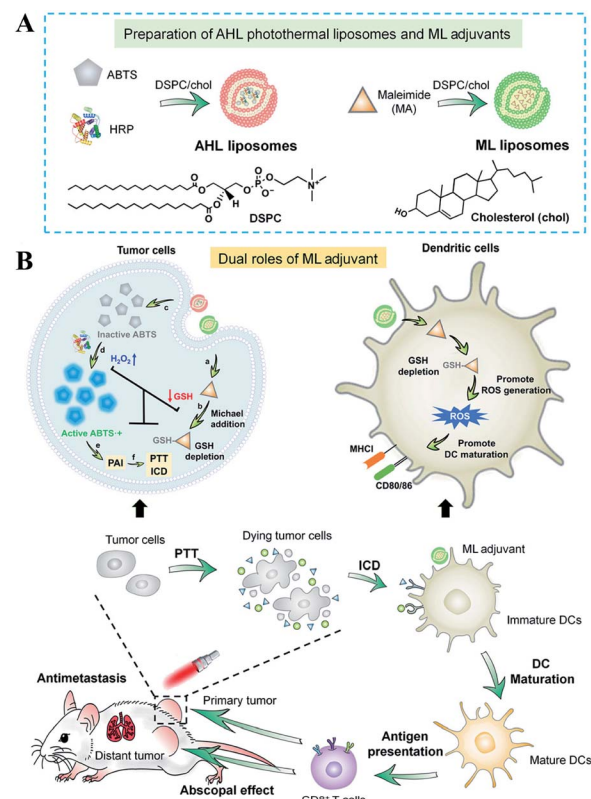


Fig. 12 Schematic illustrations of the design (A) and application (B) of the AHL photothermal liposomes and ML adjuvants. Maleimide induced the depletion of GSH causing RDH, which enhanced the photothermal immunotherapy of breast cancer through promoting immunogenic cell death (ICD). Adapted from ref. 76 with permission. Copyright 2020 American Association for the Advancement of Science.

(HES-OA) nanoparticles with PEITC for potent PDT. GSH depletion by PEITC led to the imbalance of redox homeostasis in tumor cells and significantly enhanced ICG-based PDT. Furthermore, Guangjun Nie *et al.* utilized another naturally occurring compound, sulforaphane (SFN), stemming from broccoli, to deplete GSH *via* directly forming the GSH-SFN complex, which could be exported outside cells and result in disrupting tumor redox homeostasis.<sup>78</sup> Based on this, the authors constructed a codelivery system to simultaneously encapsulate two drugs, anticancer agent cisplatin (*cis*-dichlorodiammineplatinum(II), CDDP) and SFN. The use of SFN greatly improved the therapeutic efficacy of platinum (Pt)-based chemotherapy.

### 3.3 Decreasing other reducing species to realize RDH

Besides GSH, the thioredoxin/thioredoxin reductase (Trx/TrxR) system in cancer is another important antioxidant defense system.<sup>79</sup> TrxR, which is the major disulfide reductase, can reduce the disulfide of oxidized Trx (Trx-S<sub>2</sub>) to a dithiol (Trx-SH)<sub>2</sub>. It has been reported that Au nanoclusters could effectively inhibit TrxR in the tumor cell cytoplasm. Xueyun Gao *et al.* constructed spatiotemporal controllable liposomal



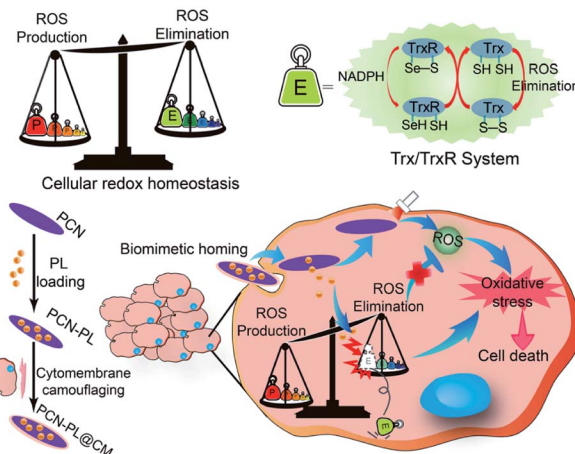


Fig. 13 Schematic illustration of interfering with the TrxR pathway in cancer cells for improved PDT. The released PL from PCN could effectively inhibit TrxR-mediated  $\text{H}_2\text{O}_2$  elimination to disturb cellular redox homeostasis, improving the MOF-mediated PDT efficacy. Adapted from ref. 81 with permission. Copyright 2019 Elsevier.

nanocomposites, co-loaded with Au nanoclusters and photosensitizer Chlorine 6 (Ce6).<sup>80</sup> Au nanoclusters effectively inhibited TrxR to induce RDH, which enhanced the Ce6-mediated PDT efficacy. Similarly, Xianzheng Zhang *et al.* reported a porous MOF of Zirconium-metallocporphyrin PCN-22 (PCN), loaded with a TrxR inhibitor alkaloid piperlongumine (PL).<sup>81</sup> Inside tumor cells, the released PL could effectively inhibit TrxR-mediated  $\text{H}_2\text{O}_2$  elimination to disturb cellular redox homeostasis, improving the PDT efficacy (Fig. 13).

## 4. Regulation of both reducing and oxidizing species to realize RDH

In addition to single regulation of oxidizing species or reducing species in cells, simultaneous regulation of both oxidizing species and reducing species to realize RDH has also been widely developed. Compared with single regulation, simultaneous regulation of both of them may induce a faster and higher degree of RDH. Therefore, this “Two-way regulation” strategy has been widely used in various cancer therapeutic regimens including PDT, SDT, CDT, RT, starvation therapy, chemotherapy, immunotherapy, and ferroptosis. Currently, this section is divided into two groups: (1) two-way regulated RDH combined with monotherapy, and (2) two-way regulated RDH combined with combinational therapies.

### 4.1 Two-way regulated-RDH combined with monotherapy

To enhance the PDT efficiency, Xianzheng Zhang *et al.* constructed SRF@Fe(<sup>III</sup>)TA nanoparticles in which  $\text{Fe}^{3+}$  and tannic acid (TA) spontaneously formed a network-like corona onto sorafenib (SRF) nanocores.<sup>82</sup> TA was arranged to chemically reduce  $\text{Fe}^{3+}$  to  $\text{Fe}^{2+}$ , inducing a Fenton-like reaction to produce cytotoxic oxidizing species  $\cdot\text{OH}$ . Meanwhile, SRF can deactivate glutathione peroxidase 4 (GPX4) to block cellular antioxidant defense. Both of the above processes disrupted the redox

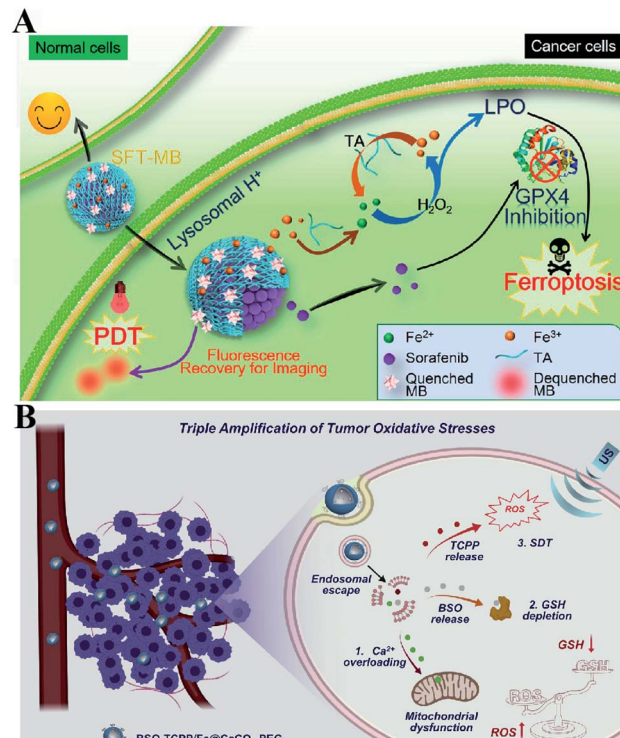


Fig. 14 Schematic illustration of two-way regulated-RDH combined with (A) PDT and (B) SDT. (A) SRF@Fe(<sup>III</sup>)TA nanoparticles for RDH-sensitized PDT. TA is arranged to induce a Fenton-like reaction to produce cytotoxic  $\cdot\text{OH}$ . Meanwhile, SRF can deactivate GPX4 to block cellular antioxidant defense. Adapted from ref. 82 with permission. Copyright 2018 American Chemical Society. (B) BSO-TCPP/Fe@CaCO<sub>3</sub> nanoparticles for RDH-sensitized SDT. Ca<sup>2+</sup>-overloading-induced ROS generation and BSO-induced GSH depletion led to RDH, enhancing TCPP-mediated SDT. Adapted from ref. 83 with permission. Copyright 2020 Elsevier.

homeostasis of tumor cells, enhancing photosensitizer methylene blue (MB)-induced PDT (Fig. 14A). To promote the SDT efficiency, Zhuang Liu *et al.* utilized CaCO<sub>3</sub> nanoparticles as the template to obtain pH-dissociable hollow metal-organic coordination nanostructures, where *meso*-tetra-(4-carboxyphenyl) porphine (TCPP) and ferric ions were chosen as the sono-sensitizer and metallic center, respectively.<sup>83</sup> Upon endocytosis by tumor cells, the nanocomplex could fast dissociate to release Ca<sup>2+</sup> and BSO. The released Ca<sup>2+</sup> remarkably elevated intracellular Ca<sup>2+</sup> concentrations and resulted in mitochondria damage, which then induced severe ROS production and subsequently synergized with BSO-mediated GSH depletion to cause RDH. This strategy ultimately enhanced TCPP-mediated SDT (Fig. 14B). For starvation therapy,<sup>84,85</sup> Xiu Jiang *et al.* presented a GOx-loaded nanozyme IrOx-GOx, which can convert H<sub>2</sub>O<sub>2</sub> at tumor tissues to O<sub>2</sub>, which could further react with glucose to produce H<sub>2</sub>O<sub>2</sub> by using GOx.<sup>86</sup> IrOx not only can generate O<sub>2</sub> and  $\cdot\text{OH}$  by its gluconic acid-unlocked oxidase and peroxidase-like activities, but also can consume GSH through its self-cyclic valence alteration of Ir(<sup>IV</sup>) and Ir(<sup>III</sup>). Consequently, introduction of this as-prepared nanozyme into tumor cells could cause RDH, enhancing GOx-induced starvation therapy

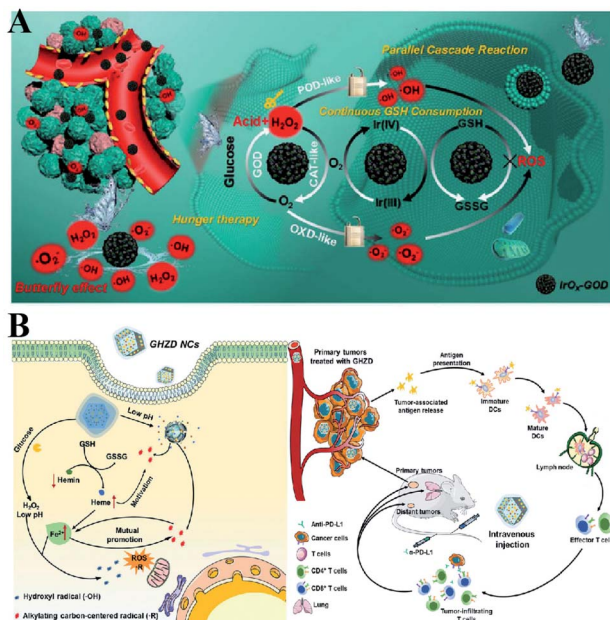


Fig. 15 (A) Schematic illustration of two-way regulation leading to RDH, sensitizing GOx-induced starvation therapy. Adapted from ref. 86 with permission. Copyright 2020 Wiley-VCH. (B) Two-way regulation led to RDH, sensitizing PD-L1-mediated immunotherapy. Adapted from ref. 93 with permission. Copyright 2020 Wiley-VCH.

(Fig. 15A). For immunotherapy<sup>87–92</sup> Jun Lin *et al.* reported an artificial cascade enzyme–drug conjugate (GHZD NCs), in which GOx, ferric protoporphyrin (Hemin), and dihydroartemisinin (DHA) were automatically localized into zeolitic imidazolate framework-8 (ZIF-8) scaffolds *via* a one-pot reaction. GOx catalyzed glucose to produce  $\text{H}_2\text{O}_2$ .<sup>93</sup> Moreover, hemin ( $\text{Fe}^{3+}$ ) acted as not only peroxidase producing  $\text{OH}^-$ , but also glutathione peroxidase consuming antioxidant GSH, resulting in the

destruction of redox homeostasis. Consequently,  $\text{Fe}^{3+}$  would be converted to  $\text{Fe}^{2+}$ , which sequentially triggered the drug DHA to burst C-centered free radicals. All the above processes amplified the immunogenic cell death effect and combated immunosuppressive tumors (Fig. 15B).

Two-way regulated-RDH strategies have been widely developed to enhance the CDT efficiency.<sup>94</sup> Our group synthesized FeCysPW@ZIF-82@CAT Dz nanoparticles<sup>13</sup> in which the shell ZIF-82 can be degraded into  $\text{Zn}^{2+}$  as a cofactor for catalase DNAzyme (CAT Dz) mediated CAT silencing and the electrophilic ligand for GSH depletion. This two-way regulation could induce RDH, sensitizing tumor cells to FeCysPW-induced CDT (Fig. 16A). To further enhance the efficacy of CDT, our group constructed DMON@Fe<sup>0</sup>/AT nanoparticles.<sup>95</sup> On one hand, S-S bond-rich dendritic mesoporous organic silica (DMON) could decrease the content of GSH in tumor cells. On the other hand, the catalase inhibitor (3-amino-1,2,4-triazole (AT)) could suppress the activity of catalase for  $\text{H}_2\text{O}_2$  accumulation. DMON@Fe<sup>0</sup>/AT can effectively inhibit the expression of ferroportin 1 to disrupt the cellular iron metabolism system, leading to the retention of iron in the cytoplasm for CDT. With DMON-mediated GSH-depletion and AT-mediated  $\text{H}_2\text{O}_2$  production, DMON@Fe<sup>0</sup>/AT would dramatically induce RDH in tumor cells to enhance the CDT efficacy (Fig. 16B). This RDH-sensitized CDT strategy was also performed by other groups. For example, Xiaogang Qu *et al.* designed a nanosystem PZIF67-AT by modifying 3-AT and PEG on zeolitic imidazole framework-67 (ZIF-67) nanoparticles that were formed by bridging 2-methylimidazole (2-mim) and cobalt ions with a sodalite zeolite-type topology.<sup>96</sup> This system not only displayed SOD-like activity capable of converting  $\text{O}_2^-$  to  $\text{H}_2\text{O}_2$ , but also could deplete GSH *via* catalase inhibitor AT, which led to an accumulation of  $\text{H}_2\text{O}_2$ . The above processes would ultimately cause RDH and intensify the Fenton-like reaction-based CDT. Furthermore, Guanbin Song *et al.* constructed  $\beta$ -lapachone (Lapa)-loaded iron oxide

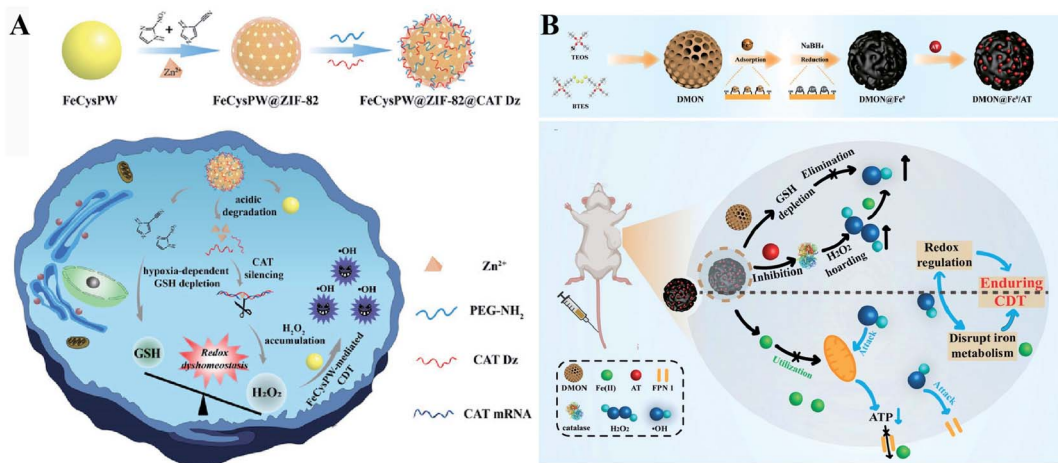


Fig. 16 Schematic illustration of two-way regulated-RDH strategies to enhance the CDT efficiency. (A) The design and multiple functions of FeCysPW@ZIF-82@CAT Dz nanoparticles. The shell ZIF-82 can be degraded into  $\text{Zn}^{2+}$  as a cofactor for CAT Dz mediated CAT silencing and the electrophilic ligand for GSH depletion, leading to RDH, sensitizing FeCysPW-induced CDT. Adapted from ref. 13 with permission. Copyright 2020 Wiley-VCH. (B) The design and application of DMON@Fe<sup>0</sup>/AT. DMON-mediated GSH-depletion and AT-mediated  $\text{H}_2\text{O}_2$  production induced RDH in tumor cells sensitizing CDT efficacy. Adapted from ref. 95 with permission. Copyright 2021 Wiley-VCH.



nanocarriers ( $\text{Fe}_3\text{O}_4\text{-HSA@Lapa}$ ).<sup>97</sup> The release of Lapa selectively increased the generation of  $\text{H}_2\text{O}_2$  via NADPH:NQO1 catalysis. Meanwhile, Lapa severely consumed intracellular NADPH, leading to the inhibition of GSSG to GSH catalyzed by glutathione reductase. Therefore, Lapa not only supplied sufficient  $\text{H}_2\text{O}_2$  but also inhibited GSH levels, causing RDH. Ultimately, this strategy boosted the efficiency of CDT.

#### 4.2 Two-way regulated-RDH combined with combinational therapies

It is well established that monotherapy is less effective than combinational therapies. Therefore, the two-way regulated-RDH could be used to further strengthen the combinational therapy, which has received tremendous attention. Peng Huang

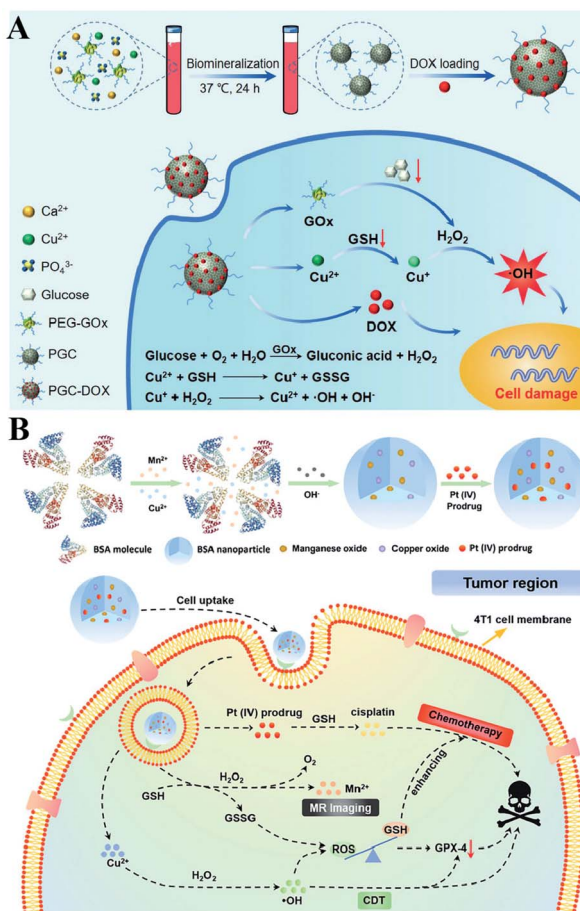


**Fig. 17** Schematic illustrations of the two-way regulation combining chemotherapy and CDT. (A) Synthetic process and function of PGC-DOX. GOx can effectively catalyze intracellular glucose to generate  $\text{H}_2\text{O}_2$ . Meanwhile, the released  $\text{Cu}^{2+}$  ions could react with GSH and induce GSH depletion. This two-way regulation led to RDH sensitizing  $\text{Cu}^{+}$ -induced CDT and DOX-mediated chemotherapy. Adapted from ref. 98 with permission. Copyright 2021 Wiley-VCH. (B) Synthetic process and function of CMBP NPs. Copper species can catalyze  $\text{H}_2\text{O}_2$  to produce  $\cdot\text{OH}$  by a Fenton-like reaction, while  $\text{MnO}_x$  can react with GSH, leading to the GSH depletion. This two-way regulation gave rise to the disruption of redox homeostasis, which promoted better chemotherapy and CDT efficacies. Adapted from ref. 99 with permission. Copyright 2021 Wiley-VCH.

*et al.* used PEG-modified GOx as a template to construct biodegradable copper-doped calcium phosphate nanoparticles, followed by the loading of doxorubicin (DOX), named PGC-DOX. GOx could effectively catalyze intracellular glucose to produce  $\text{H}_2\text{O}_2$ .<sup>98</sup> Meanwhile, the released  $\text{Cu}^{2+}$  ions could react with GSH and induce GSH depletion.  $\text{Cu}^{2+}$  could simultaneously be reduced to Fenton agent  $\text{Cu}^{+}$  ions. The above processes would ultimately perturb redox homeostasis, resulting in enhanced  $\text{Cu}^{+}$ -induced CDT and DOX-mediated chemotherapy (Fig. 17A). Similarly, Hangrong Chen *et al.* constructed a novel albumin-based multifunctional nanoagent, in which CuO and  $\text{MnO}_x$  *in situ* grew inside the bovine serum albumin (BSA) through a facile biomimetic process, followed by the conjugation of the Pt(iv) prodrug to obtain the final nanoagent.<sup>99</sup> In this system, copper species can catalyze  $\text{H}_2\text{O}_2$  to produce  $\cdot\text{OH}$  by a Fenton-like reaction, while  $\text{MnO}_x$  can react with GSH, leading to the GSH depletion.  $\cdot\text{OH}$  accumulation and GSH depletion gave rise to a disruption of redox homeostasis, which promoted better chemotherapy and CDT efficacies (Fig. 17B).

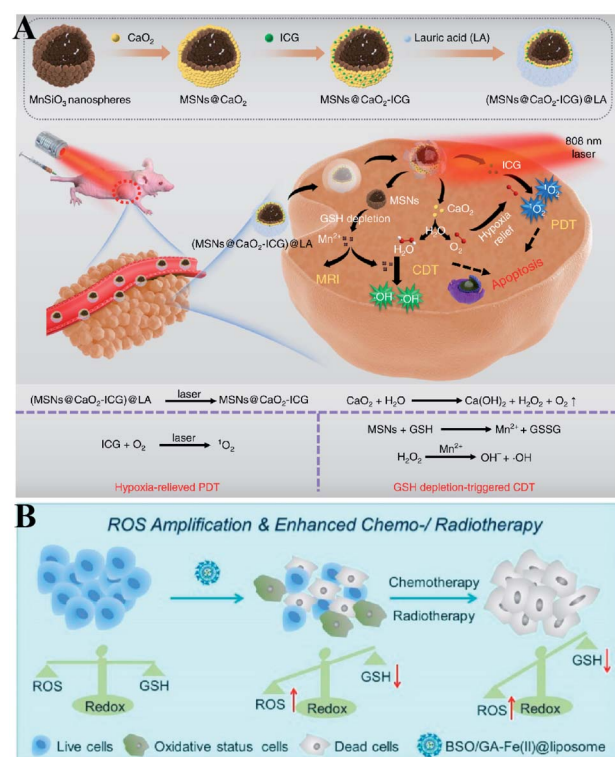


**Fig. 18** Two-way regulated-RDH combined with combinational therapies. (A) Schematic illustrations of the synthetic process and function of (MSNs@CaO<sub>2</sub>-ICG)@LA NPs. This system can induce redox homeostasis, which enhanced the efficacies of PDT and CDT. Adapted from ref. 100 with permission. Copyright 2020 Nature Publishing Group. (B) Schematic illustrations of the function of BSO/GA-Fe(II)@liposome. GA-Fe(II)-mediated  $\cdot\text{OH}$  production and BSO-mediated GSH depletion dramatically induced RDH in tumor cells, which then resulted in remarkably improved therapeutic efficacies of concurrently applied chemotherapy or RT. Adapted from ref. 101 with permission. Copyright 2019 American Chemical Society.



Furthermore, Haifeng Dong *et al.* reported an  $\text{H}_2\text{O}_2/\text{O}_2$  self-supplying nanoagent (MSNs@ $\text{CaO}_2$ -ICG)@LA.<sup>100</sup> Under laser irradiation, ICG simultaneously generated singlet oxygen and emitted heat to melt the phase-change material lauric acid (LA). The exposed  $\text{CaO}_2$  reacted with water to rapidly generate  $\text{H}_2\text{O}_2$  and  $\text{O}_2$ . The interaction between MSNs and GSH led to the release of  $\text{Mn}^{2+}$  and GSH depletion. Thus, this system could accumulate  $\text{H}_2\text{O}_2$  and eliminate GSH to destroy redox homeostasis, which enhanced the efficacies of PDT and CDT (Fig. 18A). To further promote the efficiency of SDT-induced tumor therapy, Zhuang Liu *et al.* synthesized new nanomaterials to combine RDH with chemotherapy and radiotherapy. Gallic acid-ferrous (GA-Fe(II)) and BSO were co-encapsulated within liposome (BSO/GA-Fe(II)@liposome).<sup>101</sup> GA-Fe(II) nanocomplexes were used as the catalyst of Fenton reaction to enable persistent conversion of  $\text{H}_2\text{O}_2$  to highly cytotoxic hydroxyl radicals ( $\cdot\text{OH}$ ), leading to the increase of oxidizing species. Meanwhile, the released BSO could inhibit the biosynthesis of GSH, resulting in the decrease of reducing species. Thus, GA-Fe(II)-mediated  $\cdot\text{OH}$  production and BSO-mediated GSH depletion would dramatically enhance RDH in tumor cells, which then resulted in remarkably improved therapeutic efficacies of concurrently applied chemotherapy or radiotherapy (Fig. 18B).

## 5. Conclusions and perspectives

This review summarizes the current progress of RDH for tumor therapy. This strategy focuses on the use of nanomaterials to disturb redox homeostasis by regulating intracellular oxidizing states, reducing states or both of them at the same time, which increases the sensitivity of tumor cells to various therapeutic modalities. Although nanomaterial-mediated RDH has been widely applied in the research of tumor therapy, many important scientific problems still need to be considered before it is ready for clinical transformation.

First, it is critically vital to deeply explore cellular biological mechanisms involved in redox homeostasis, which is beneficial to further optimize the RDH strategy at the genetic and molecular levels. Second, redox homeostasis is ubiquitous in various cells.<sup>102,103</sup> Thus, it is necessary to make tumor cells more specific and sensitive for the RDH strategy, avoiding potential toxic and side effects on normal tissues and organs. Finally, the most important issue is to improve the efficacy of RDH strategy-mediated tumor treatment. At present, most of the tumor treatments are based on ROS-mediated oxidative stress to kill tumor cells. In view of the resistance of tumor cells to ROS-mediated therapy, some new tumor therapeutic modalities could be combined with RDH. On the one hand, there is an urgent need to explore novel active species other than ROS/RNS, such as alkyl radicals ( $\text{R}^\bullet$ )<sup>104,105</sup> or chlorine radicals ( $\cdot\text{Cl}$ ),<sup>106</sup> which may exhibit higher efficacy in tumor treatment. On the other hand, reductive stress attracts increasing attention,<sup>107</sup> which could break through the bottleneck of existing oxidative stress-mediated tumor treatment.

In summary, the RDH strategy, as a research hotspot in the field of tumor therapy, has attracted increasing attention of worldwide researchers, despite the existence of some unresolved

issues. Under the guidance of the RDH strategy, researchers are still exploring various novel nanomaterials for accurate regulation of redox homeostasis to enhance tumor therapy efficacy. We expect that the development of the RDH strategy will not only provide valuable insights for the design of various functional nanomaterials, but also bring more breakthroughs in the treatment of cancer or other diseases in the future.

## Author contributions

Y. L. Wu and Y. L. Li contributed equally to this work. All authors participated in this review work. Y. L. Wu, Y. L. Li and W. B. Bu conceived the structure of this review. Y. L. Wu, Y. L. Li and G. L. Lv prepared the draft. G. L. Lv and W. B. Bu reviewed and refined the manuscript.

## Conflicts of interest

There are no conflicts to declare.

## Acknowledgements

The authors would greatly acknowledge the financial support by the National Funds for Distinguished Young Scientists (Grant No. 51725202), the Key Project of Shanghai Science and Technology Commission (Grant No. 19JC1412000), and the National Natural Science Foundation of China (Grant No. 51872094, 82172091).

## References

- 1 P. H. G. M. Willems, R. Rossignol, C. E. J. Dieteren, M. P. Murphy and W. J. H. Koopman, *Cell Metab.*, 2015, **22**, 207–218.
- 2 G. S. Shadel and T. L. Horvath, *Cell*, 2015, **163**, 560–569.
- 3 N. T. Moldogazieva, I. M. Mokhosoev, N. B. Feldman and S. V. Lutsenko, *Free Radical Res.*, 2018, **52**, 507–543.
- 4 A. Ghoneum, A. Y. Abdulfattah, B. O. Warren, J. Shu and N. Said, *Int. J. Mol. Sci.*, 2020, **21**, 3100.
- 5 D. Samanta and G. L. Semenza, *Redox Biol.*, 2017, **13**, 331–335.
- 6 D. Trachootham, J. Alexandre and P. Huang, *Nat. Rev. Drug Discovery*, 2009, **8**, 579–591.
- 7 D. S. A. Simpson and P. L. Oliver, *Antioxidants*, 2020, **9**, 743.
- 8 E. Panieri and M. M. Santoro, *Cell Death Dis.*, 2016, **7**, e2253.
- 9 B. Marengo, M. Nitti, A. L. Furfaro, R. Colla, C. D. Ciucis, U. M. Marinari, M. A. Pronzato, N. Traverso and C. Domenicotti, *Oxid. Med. Cell. Longevity*, 2016, **2016**, 6235641.
- 10 D. H. Hyun, *Cancers*, 2020, **12**, 1822.
- 11 T. C. Jorgenson, W. Zhong and T. D. Oberley, *Cancer Res.*, 2013, **73**, 6118–6123.
- 12 C. L. Grek and K. D. Tew, *Curr. Opin. Pharmacol.*, 2010, **10**, 362–368.
- 13 Y. Li, P. Zhao, T. Gong, H. Wang, X. Jiang, H. Cheng, Y. Liu, Y. Wu and W. Bu, *Angew. Chem., Int. Ed.*, 2020, **59**, 22537–22543.



14 L. Kou, X. Jiang, H. Huang, X. Lin, Y. Zhang, Q. Yao and R. Chen, *Asian J. Pharm. Sci.*, 2020, **15**, 145–157.

15 R. P. Brandes, N. Weissmann and K. Schroeder, *Free Radical Biol. Med.*, 2014, **76**, 208–226.

16 T. Itoh, R. Terazawa, K. Kojima, K. Nakane, T. Deguchi, M. Ando, Y. Tsukamasa, M. Ito and Y. Nozawa, *Free Radical Res.*, 2011, **45**, 1033–1039.

17 P. Ma, H. Xiao, C. Yu, J. Liu, Z. Cheng, H. Song, X. Zhang, C. Li, J. Wang, Z. Gu and J. Lin, *Nano Lett.*, 2017, **17**, 928–937.

18 M. Huo, L. Wang, Y. Chen and J. Shi, *Nat. Commun.*, 2017, **8**, 357.

19 K. Chang, Z. Liu, X. Fang, H. Chen, X. Men, Y. Yuan, K. Sun, X. Zhang, Z. Yuan and C. Wu, *Nano Lett.*, 2017, **17**, 4323–4329.

20 J. Tang, A. K. Meka, S. Theivendran, Y. Wang, Y. Yang, H. Song, J. Fu, W. Ban, Z. Gu, C. Lei, S. Li and C. Yu, *Angew. Chem., Int. Ed.*, 2020, **59**, 22054–22062.

21 Z. Zhuang, J. Dai, M. Yu, J. Li, P. Shen, R. Hu, X. Lou, Z. Zhao and B. Z. Tang, *Chem. Sci.*, 2020, **11**, 3405–3417.

22 M. Li, J. Xia, R. Tian, J. Wang, J. Fan, J. Du, S. Long, X. Song, J. W. Foley and X. Peng, *J. Am. Chem. Soc.*, 2018, **140**, 14851–14859.

23 K. Zhang, Z. Yu, X. Meng, W. Zhao, Z. Shi, Z. Yang, H. Dong and X. Zhang, *Adv. Sci.*, 2019, **6**, 1900530.

24 S. K. Parks, J. Chiche and J. Pouyssegur, *Nat. Rev. Cancer*, 2013, **13**, 611–623.

25 V. L. Payen, E. Mina, V. F. Van Hee, P. E. Porporato and P. Sonveaux, *Mol. Metabol.*, 2020, **33**, 48–66.

26 Y. Liu, X. Ji, W. W. L. Tong, D. Askhatova, T. Yang, H. Cheng, Y. Wang and J. Shi, *Angew. Chem., Int. Ed.*, 2018, **57**, 1510–1513.

27 L. Sun, Y. Xu, Y. Gao, X. Huang, S. Feng, J. Chen, X. Wang, L. Guo, M. Li, X. Meng, J. Zhang, J. Ge, X. An, D. Ding, Y. Luo, Y. Zhang, Q. Jiang and X. Ning, *Small*, 2019, **15**, e1901156.

28 W.-P. Li, C.-H. Su, Y.-C. Chang, Y.-J. Lin and C.-S. Yeh, *ACS Nano*, 2016, **10**, 2017–2027.

29 X. Song, J. Xu, C. Liang, Y. Chao, Q. Jin, C. Wang, M. Chen and Z. Liu, *Nano Lett.*, 2018, **18**, 6360–6368.

30 M. Zhang, B. Shen, R. Song, H. Wang, B. Lv, X. Meng, Y. Liu, Y. Liu, X. Zheng, W. Su, C. Zuo and W. Bu, *Mater. Horiz.*, 2019, **6**, 1034–1040.

31 Z. Tang, Y. Liu, D. Ni, J. Zhou, M. Zhang, P. Zhao, B. Lv, H. Wang, D. Jin and W. Bu, *Adv. Mater.*, 2020, **32**, e1904011.

32 L. S. Lin, T. Huang, J. Song, X. Y. Ou, Z. Wang, H. Deng, R. Tian, Y. Liu, J. F. Wang, Y. Liu, G. Yu, Z. Zhou, S. Wang, G. Niu, H. H. Yang and X. Chen, *J. Am. Chem. Soc.*, 2019, **141**, 9937–9945.

33 M. Zhang, R. Song, Y. Liu, Z. Yi, X. Meng, J. Zhang, Z. Tang, Z. Yao, Y. Liu, X. Liu and W. Bu, *Chem.*, 2019, **5**, 2171–2182.

34 W. Fan, W. Bu, Z. Zhang, B. Shen, H. Zhang, Q. He, D. Ni, Z. Cui, K. Zhao, J. Bu, J. Du, J. Liu and J. Shi, *Angew. Chem., Int. Ed.*, 2015, **54**, 14026–14030.

35 M. Wang, Z. Hou, S. Liu, S. Liang, B. Ding, Y. Zhao, M. Chang, G. Han, A. A. A. Kheraif and J. Lin, *Small*, 2021, **17**, e2005728.

36 B. Poljsak, D. Suput and I. Milisav, *Oxid. Med. Cell. Longevity*, 2013, **2013**, 956792.

37 A. Glasauer and N. S. Chandel, *Biochem. Pharmacol.*, 2014, **92**, 90–101.

38 L. He, T. He, S. Farrar, L. Ji, T. Liu and X. Ma, *Cell. Physiol. Biochem.*, 2017, **44**, 532–553.

39 C. Gorrini, I. S. Harris and T. W. Mak, *Nat. Rev. Drug Discovery*, 2013, **12**, 931–947.

40 A. V. Snezhkina, A. V. Kudryavtseva, O. L. Kardymon, M. V. Savvateeva, N. V. Melnikova, G. S. Krasnov and A. A. Dmitriev, *Oxid. Med. Cell. Longevity*, 2019, **2019**, 1–16.

41 C. Zhang, W. Bu, D. Ni, C. Zuo, C. Cheng, Q. Li, L. Zhang, Z. Wang and J. Shi, *J. Am. Chem. Soc.*, 2016, **138**, 8156–8164.

42 B. Niu, K. Liao, Y. Zhou, T. Wen, G. Quan, X. Pan and C. Wu, *Biomaterials*, 2021, **277**, 121110.

43 Y. Xiong, C. Xiao, Z. Li and X. Yang, *Chem. Soc. Rev.*, 2021, **50**, 6013–6041.

44 S. C. Lu, *Biochim. Biophys. Acta*, 2013, **1830**, 3143–3153.

45 S. J. Kim, H. G. Kim, B. C. Kim, K. Kim, E. H. Park and C. J. Lim, *J. Microbiol.*, 2004, **42**, 233–238.

46 S.-O. Kang and M.-K. Kwak, *J. Microbiol. Biotechnol.*, 2021, **31**, 79–91.

47 I. S. Harris, A. E. Treloar, S. Inoue, M. Sasaki, C. Gorrini, K. C. Lee, K. Y. Yung, D. Brenner, C. B. Knobbe-Thomsen, M. A. Cox, A. Elia, T. Berger, D. W. Cescon, A. Adeoye, A. Bruestle, S. D. Molyneux, J. M. Mason, W. Y. Li, K. Yamamoto, A. Wakeham, H. K. Berman, R. Khokha, S. J. Done, T. J. Kavanagh, C.-W. Lam and T. W. Mak, *Cancer Cell*, 2015, **27**, 211–222.

48 H. Sun, M. Feng, S. Chen, R. Wang, Y. Luo, B. Yin, J. Li and X. Wang, *J. Mater. Chem. B*, 2020, **8**, 7149–7159.

49 X. Guan, H. H. Yin, X. H. Xu, G. Xu, Y. Zhang, B. G. Zhou, W. W. Yue, C. Liu, L. P. Sun, H. X. Xu and K. Zhang, *Adv. Funct. Mater.*, 2020, **30**, 2000326.

50 S. B. Gunnoo and A. Madder, *ChemBioChem*, 2016, **17**, 529–553.

51 C. E. Paulsen and K. S. Carroll, *Chem. Rev.*, 2013, **113**, 4633–4679.

52 A. Bansal and M. C. Simon, *J. Cell Biol.*, 2018, **217**, 2291–2298.

53 L. Kou, R. Sun, S. Xiao, Y. Zheng, Z. Chen, A. Cai, H. Zheng, Q. Yao, V. Ganapathy and R. Chen, *ACS Appl. Mater. Interfaces*, 2019, **11**, 26722–26730.

54 H. Tang, C. Li, Y. Zhang, H. Zheng, Y. Cheng, J. Zhu, X. Chen, Z. Zhu, J. G. Piao and F. Li, *Theranostics*, 2020, **10**, 9865–9887.

55 L. Wang, Y. Liu, T. Du, H. Yang, L. Lei, M. Guo, H. F. Ding, J. Zhang, H. Wang, X. Chen and C. Yan, *Cell Death Differ.*, 2020, **27**, 662–675.

56 L. Sleire, B. S. Skeie, I. A. Netland, H. E. Forde, E. Dodoo, F. Selheim, L. Leiss, J. I. Heggdal, P. H. Pedersen, J. Wang and P. O. Enger, *Oncogene*, 2015, **34**, 5951–5959.

57 E. Lachaier, C. Louandre, C. Godin, Z. Saidak, M. Baert, M. Diouf, B. Chauffert and A. Galmiche, *Anticancer Res.*, 2014, **34**, 6417–6422.

58 Y. S. Chang, J. Adnane, P. A. Trail, J. Levy, A. Henderson, D. Xue, E. Bortolon, M. Ichetovkin, C. Chen, A. McNabola,



D. Wilkie, C. A. Carter, I. C. A. Taylor, M. Lynch and S. Wilhelm, *Cancer Chemother. Pharmacol.*, 2007, **59**, 561–574.

59 L. Jiang, N. Kon, T. Li, S. J. Wang, T. Su, H. Hibshoosh, R. Baer and W. Gu, *Nature*, 2015, **520**, 57–62.

60 D. W. Zheng, Q. Lei, J. Y. Zhu, J. X. Fan, C. X. Li, C. Li, Z. Xu, S. X. Cheng and X. Z. Zhang, *Nano Lett.*, 2017, **17**, 284–291.

61 X. Guo, F. Liu, J. Deng, P. Dai, Y. Qin, Z. Li, B. Wang, A. Fan, Z. Wang and Y. Zhao, *ACS Nano*, 2020, **14**, 14715–14730.

62 L. S. Pike, A. L. Smift, N. J. Croteau, D. A. Ferrick and M. Wu, *Biochim. Biophys. Acta*, 2011, **1807**, 726–734.

63 H. Fan, G. Yan, Z. Zhao, X. Hu, W. Zhang, H. Liu, X. Fu, T. Fu, X. B. Zhang and W. Tan, *Angew. Chem., Int. Ed.*, 2016, **55**, 5477–5482.

64 J. Ou, H. Tian, J. Wu, J. Gao, J. Jiang, K. Liu, S. Wang, F. Wang, F. Tong, Y. Ye, L. Liu, B. Chen, X. Ma, X. Chen, F. Peng and Y. Tu, *ACS Appl. Mater. Interfaces*, 2021, **13**, 38050–38060.

65 L.-S. Lin, J. Song, L. Song, K. Ke, Y. Liu, Z. Zhou, Z. Shen, J. Li, Z. Yang, W. Tang, G. Niu, H.-H. Yang and X. Chen, *Angew. Chem., Int. Ed.*, 2018, **57**, 4902–4906.

66 H. He, Q. Yang, H. Li, S. Meng, Z. Xu, X. Chen, Z. Sun, B. Jiang and C. Li, *Microchim. Acta*, 2021, **188**, 141.

67 L.-S. Lin, J. Song, L. Song, K. Ke, Y. Liu, Z. Zhou, Z. Shen, J. Li, Z. Yang, W. Tang, G. Niu, H.-H. Yang and X. Chen, *Angew. Chem., Int. Ed.*, 2018, **57**, 4902–4906.

68 C. Liu, D. Wang, S. Zhang, Y. Cheng, F. Yang, Y. Xing, T. Xu, H. Dong and X. Zhang, *ACS Nano*, 2019, **13**, 4267–4277.

69 M. Chang, M. Wang, M. Wang, M. Shu, B. Ding, C. Li, M. Pang, S. Cui, Z. Hou and J. Lin, *Adv. Mater.*, 2019, **31**, 1905271.

70 L.-H. Fu, Y. Wan, C. Qi, J. He, C. Li, C. Yang, H. Xu, J. Lin and P. Huang, *Adv. Mater.*, 2021, **33**, 2006892.

71 B. Ma, S. Wang, F. Liu, S. Zhang, J. Duan, Z. Li, Y. Kong, Y. Sang, H. Liu, W. Bu and L. Li, *J. Am. Chem. Soc.*, 2019, **141**, 849–857.

72 Y. Yong, C. Zhang, Z. Gu, J. Du, Z. Guo, X. Dong, J. Xie, G. Zhang, X. Liu and Y. Zhao, *ACS Nano*, 2017, **11**, 7164–7176.

73 R. Zhou, H. Wang, Y. Yang, C. Zhang, X. Dong, J. Du, L. Yan, G. Zhang, Z. Gu and Y. Zhao, *Biomaterials*, 2019, **189**, 11–22.

74 S. Her, D. A. Jaffray and C. Allen, *Adv. Drug Delivery Rev.*, 2017, **109**, 84–101.

75 X. Zhang, X. Chen, Y.-W. Jiang, N. Ma, L.-Y. Xia, X. Cheng, H.-R. Jia, P. Liu, N. Gu, Z. Chen and F.-G. Wu, *ACS Appl. Mater. Interfaces*, 2018, **10**, 10601–10606.

76 Z. Zhou, H. Wu, R. Yang, A. Xu, Q. Zhang, J. Dong, C. Qian and M. Sun, *Sci. Adv.*, 2020, **6**, eabc4373.

77 H. Hu, J. Chen, H. Yang, X. Huang, H. Wu, Y. Wu, F. Li, Y. Yi, C. Xiao, Y. Li, Y. Tang, Z. Li, B. Zhang and X. Yang, *Nanoscale*, 2019, **11**, 6384–6393.

78 Y. Xu, X. Han, Y. Li, H. Min, X. Zhao, Y. Zhang, Y. Qi, J. Shi, S. Qi, Y. Bao and G. Nie, *ACS Nano*, 2019, **13**, 13445–13455.

79 J. Zhang, X. Li, X. Han, R. Liu and J. Fang, *Trends Pharmacol. Sci.*, 2017, **38**, 794–808.

80 F. Gao, W. Zheng, L. Gao, P. Cai, R. Liu, Y. Wang, Q. Yuan, Y. Zhao and X. Gao, *Adv. Healthcare Mater.*, 2017, **6**, 1601453.

81 Q. Cheng, W. Yu, J. Ye, M. Liu, W. Liu, C. Zhang, C. Zhang, J. Feng and X. Z. Zhang, *Biomaterials*, 2019, **224**, 119500.

82 T. Liu, W. Liu, M. Zhang, W. Yu, F. Gao, C. Li, S. B. Wang, J. Feng and X. Z. Zhang, *ACS Nano*, 2018, **12**, 12181–12192.

83 Z. Dong, L. Feng, Y. Hao, Q. Li, M. Chen, Z. Yang, H. Zhao and Z. Liu, *Chem.*, 2020, **6**, 1391–1407.

84 C. Wang, J. Yang, C. Dong and S. Shi, *Adv. Ther.*, 2020, **3**, 2000110.

85 M. Wang, D. Wang, Q. Chen, C. Li, Z. Li and J. Lin, *Small*, 2019, **15**, 1903895.

86 W. Zhen, Y. Liu, W. Wang, M. Zhang, W. Hu, X. Jia, C. Wang and X. Jiang, *Angew. Chem., Int. Ed.*, 2020, **59**, 9491–9497.

87 J. Li, Y. Luo and K. Pu, *Angew. Chem., Int. Ed.*, 2021, **60**, 12682–12705.

88 L. A. Emens, *Clin. Cancer Res.*, 2018, **24**, 511–520.

89 K. Esfahani, L. Roudaia, N. Buhlaiga, S. V. Del Rincon, N. Papneja and W. H. Miller Jr, *Curr. Oncol.*, 2020, **27**, S87–S97.

90 L. A. Emens, P. A. Asciero, P. K. Darcy, S. Demaria, A. M. M. Eggemont, W. L. Redmond, B. Seliger and F. M. Marincola, *Eur. J. Cancer*, 2017, **81**, 116–129.

91 R. S. Riley, C. H. June, R. Langer and M. J. Mitchell, *Nat. Rev. Drug Discovery*, 2019, **18**, 175–196.

92 J. Nam, S. Son, K. S. Park, W. Zou, L. D. Shea and J. J. Moon, *Nat. Rev. Mater.*, 2019, **4**, 398–414.

93 Y. Zhao, X. Xiao, M. Zou, B. Ding, H. Xiao, M. Wang, F. Jiang, Z. Cheng, P. Ma and J. Lin, *Adv. Mater.*, 2021, **33**, e2006363.

94 Z. Tang, P. Zhao, H. Wang, Y. Liu and W. Bu, *Chem. Rev.*, 2021, **121**, 1981–2019.

95 Y. Liu, S. Zhai, X. Jiang, Y. Liu, K. Wang, C. Wang, M. Zhang, X. Liu and W. Bu, *Adv. Funct. Mater.*, 2021, **31**, 2010390.

96 Y. Sang, F. Cao, W. Li, L. Zhang, Y. You, Q. Deng, K. Dong, J. Ren and X. Qu, *J. Am. Chem. Soc.*, 2020, **142**, 5177–5183.

97 Q. Chen, J. Zhou, Z. Chen, Q. Luo, J. Xu and G. Song, *ACS Appl. Mater. Interfaces*, 2019, **11**, 30551–30565.

98 L. H. Fu, Y. Wan, C. Qi, J. He, C. Li, C. Yang, H. Xu, J. Lin and P. Huang, *Adv. Mater.*, 2021, **33**, e2006892.

99 K. Liang, H. Sun, Z. Yang, H. Yu, J. Shen, X. Wang and H. Chen, *Adv. Funct. Mater.*, 2021, **31**, 2100355.

100 C. Liu, Y. Cao, Y. Cheng, D. Wang, T. Xu, L. Su, X. Zhang and H. Dong, *Nat. Commun.*, 2020, **11**, 1735.

101 Z. Dong, L. Feng, Y. Chao, Y. Hao, M. Chen, F. Gong, X. Han, R. Zhang, L. Cheng and Z. Liu, *Nano Lett.*, 2019, **19**, 805–815.

102 J. Jezek, K. F. Cooper and R. Strich, *Antioxidants*, 2018, **7**, 13.

103 E.-M. Hanschmann, J. R. Godoy, C. Berndt, C. Hudemann and C. H. Lillig, *Antioxid. Redox Signaling*, 2013, **19**, 1539–1605.

104 X.-Q. Wang, F. Gao and X.-Z. Zhang, *Angew. Chem., Int. Ed.*, 2017, **56**, 9029–9033.

105 S. Wu, X. Liu, J. Ren and X. Qu, *Small*, 2019, **15**, 1904870.



106 R. Song, H. Wang, M. Zhang, Y. Liu, X. Meng, S. Zhai, 107 K.-S. Chun, D.-H. Kim and Y.-J. Surh, *Cells*, 2021, **10**, 758.  
C. Wang, T. Gong, Y. Wu, X. Jiang and W. Bu, *Angew. Chem., Int. Ed.*, 2020, **59**, 21032–21040.

